ELSEVIER

Biochimica et Biophysica Acta 1510 (2001) 278–291

BIOCHIMICA ET BIOPHYSICA ACTA
BBA

www.elsevier.com/locate/bba

Characterization of sterically stabilized cisplatin liposomes by nuclear magnetic resonance

Tal Peleg-Shulman [a], Dan Gibson [a,b], Rivka Cohen [c], Robert Abra [d], Yechezkel Barenholz [c,*]

[a] *Department of Medicinal Chemistry, School of Pharmacy, Hebrew University of Jerusalem, Jerusalem, Israel*
[b] *David R. Bloom Center for Pharmacy, Hebrew University of Jerusalem, Jerusalem, Israel*
[c] *Laboratory of Membrane and Liposome Research, Department of Biochemistry, Hebrew University-Hadassah Medical School, P.O. Box 12272, Jerusalem 91120, Israel*
[d] *ALZA Corporation, Mountain View, CA, USA*

Received 2 November 1999; received in revised form 16 October 2000; accepted 18 October 2000

Abstract

Extensive scientific efforts are directed towards finding new and improved platinum anticancer agents. A promising approach is the encapsulation of cisplatin in sterically stabilized, long circulating, PEGylated 100 nm liposomes. This liposomal cisplatin (STEALTH cisplatin, formerly known as SPI-77) shows excellent stability in plasma and has a longer circulation time, greater efficacy and lower toxicity than much free cisplatin. However, so far, the physicochemical characterization of STEALTH cisplatin has been limited to size distribution, drug-to-lipid ratio and stability. Information on the physical state of the drug in the liposome aqueous phases and the drug's interaction with the liposome membrane has been lacking. This study was aimed at filling this gap. We report a multinuclear NMR study in which several techniques have been used to assess the physical nature of cisplatin in liposomal formulations and if and to what extent the drug affects the liposome phospholipids. Since NMR detects only the soluble cisplatin in the liposomes and not the insoluble drug, combining NMR and atomic absorption data enables one to determine how much of the encapsulated drug is soluble in the intraliposomal aqueous phase. Our results indicate that almost all of the cisplatin remains intact during the loading process, and that the entire liposomal drug is present in a soluble form in the internal aqueous phase of the liposomes.

Keywords: Cisplatin; NMR; Liposome; PEG

Abbreviations: Cisplatin, *cis*-DDP, *cis*-diamminedichloroplatinum(II); transplatin, *trans*-DDP, *trans*-diamminedichloroplatinum(II); HMG, high mobility group; IXR, intrastrand cross-link recognition; hUBF, human upstream binding factor; LUV, large unilamellar vesicle(s); MLV, multilamellar vesicle(s); PEG, polyethylene glycol; ^{2000}PEG-DSPE, polyethylene-glycol (m.w.$\approx$2000)-derivatized distearoylphosphatidylethanolamine; HPC, hydrogenated phosphatidylcholine; HSPC, hydrogenated soy phosphatidylcholine; AAS, atomic absorption spectroscopy; ESR, electron spin resonance; NMR, nuclear magnetic resonance; HSQC, heteronuclear single quantum coherence; HMQC, heteronuclear multiple quantum coherence; RT, room temperature; EXAFS, extended X-ray absorption fine structure

* Corresponding author. Fax: +972-2-678-4010; E-mail: yb@cc.huji.ac.il

0005-2736/01/$ – see front matter
PII: S0005-2736(00)00359-X

1. Introduction

Since it was first discovered by Rosenberg et al. [1], cisplatin (*cis*-diamminedichloroplatinum(II), *cis*-DDP) has become one of the most widely used anticancer drugs in treating a variety of solid tumors, including testicular, head and neck, and lung tumors [2]. The cellular target of the drug is the DNA, with which it forms stable adducts that are responsible for the drug's anticancer activity [3].

The drug enters cells by passive diffusion. The lower intracellular chloride ion concentration (4 mM vs. 103 mM in the plasma) enables the drug to exchange its first chloride ligand with a water molecule, thus forming the positively charged mono-aqua species that can form covalent monofunctional adducts with the DNA (see Fig. 1). The monofunctional adduct reacts further, by substitution of its chloride ligand, to form bifunctional cross-links [4]. The major adduct formed between cisplatin and DNA is the bidentate, 1,2-intrastrand cross-link, *cis*-Pt-GG, in which *cis*-$[Pt(NH_3)_2]^{2+}$ binds two adjacent guanine N7 atoms (Fig. 1). Nuclear magnetic resonance and crystallographic studies show that the adduct formation unwinds the DNA by about $-21°$ and causes a kink of $\sim$40–58° in the duplex towards the major groove, and widens the minor groove of the platinated duplex at the lesion site [5,6]. These structural modifications may be the recognition motifs for high mobility group domains, such as HMG1, Ixr1 and hUBF, which bind *cis*-platinated DNA [7,8]. Once bound by these cellular proteins, the intrastrand cross-links are shielded from cellular repair mechanisms, resulting in cancer cells becoming more sensitive to the drug.

Platinum anticancer drugs are administered by intravenous injection, and within 1 day, 65–98% of the platinum in the blood plasma is protein bound [9,10]. The binding of cisplatin to proteins reduces the urinary excretion of platinum and causes the deposition of platinum in tissues. In addition, the binding of cisplatin to proteins and enzymes is believed to be the cause of many of the severe side effects exhibited by the drug, especially ototoxicity and nephrotoxicity [11,12]. So far, attempts to prevent neuro- and nephrotoxicity have failed.

Cisplatin has additional drawbacks, such as low solubility in aqueous solutions (7 mM, 2.10 mg/ml

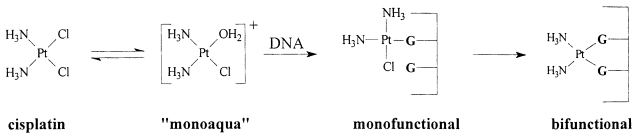

Fig. 1. Cisplatin-DNA adducts.

at 37°C), severe toxicity (i.e., nephrotoxicity, myelosuppression, central nervous system impairment) and side effects such as nausea and vomiting [13]. Acquired multi-drug resistance is known to develop in patients receiving cisplatin chemotherapy.

Although extensive efforts were devoted to overcoming these major issues by development of new generations of platinum derivatives which are less toxic and more active than cisplatin and/or do not display cross-resistance, the improvements were minimal [14]. An alternative approach is the encapsulation of cisplatin in sterically stabilized 100 nm liposomes, based on the promising animal and clinical data obtained from Doxil (a STEALTH liposomal formulation of doxorubicin HCl; ALZA Corporation, Mountain View, CA) loaded in the aqueous phase of sterically stabilized 100 nm liposomes [15,16]. Toxicity, pharmacokinetics, tissue distribution and therapeutic efficacy of cisplatin encapsulated in long circulating PEGylated liposomes were recently described [17,18]. As expected, STEALTH cisplatin has excellent stability in plasma, a much longer circulation time, better efficacy and lower toxicity than free cisplatin. However, the characterization of STEALTH cisplatin has been limited to size distribution, drug-to-lipid ratio, and stability. The physical and chemical characteristics of the drug in the liposome's aqueous phase and the drug's interaction with the liposome membrane have not been reported.

NMR is one of the most powerful tools for evaluation of liposomal formulations since the anisotropic nature of molecular motion within the lipid bilayers and the anisotropy of the membrane structure can be evaluated by this technique [19,20]. One of the major advantages of NMR applications is that the method is based on the use of intrinsic reporter moieties (the various nuclei, i.e., ^{13}C, ^{31}P, ^{1}H, ^{15}N, ^{195}Pt). Most other approaches, such as fluorescent techniques and electron spin resonance (ESR), require the use of bulky external probe moieties. In the case of cisplatin-loaded liposomes, NMR provides important information both on the liposome

phospholipids (physical state, rate of motion) and on the platinum complex (oxidation state and coordination sphere). The combination of NMR and atomic absorption spectroscopy (AAS) can be used to quantify the amount of soluble platinum in the liposome formulations.

We report a multinuclear NMR study in which several techniques were used to assess (a) the physical and chemical nature of cisplatin in liposomal formulations and (b) the extent to which the drug affects liposome phospholipids.

2. Experimental procedures

2.1. Preparation and characterization of ^{15}N-labeled cisplatin (cis-Pt($^{15}NH_3$)$_2$Cl$_2$)

cis-^{15}N-Diamminedichloroplatinum(II) (cisplatin) was synthesized according to the procedure described by Boreham et al. [19]. The product was characterized by both ^{195}Pt NMR spectroscopy and by the thiourea test. Thiourea was added to an aqueous solution of the ^{15}N-labeled cisplatin, and the solution was heated to 40–50°C. The appearance of a yellow color is indicative that the product is in the *cis* configuration, whereas the appearance of a colorless solution indicates the presence of the *trans* isomer.

The *cis*-^{15}N-DDP was dissolved in dimethylformamide (DMF) and analyzed by ^{195}Pt NMR.

2.2. Preparation of liposomes containing cisplatin

2.2.1. Preparation of ^{15}N-cisplatin encapsulated in sterically stabilized liposomes (STEALTH cisplatin)

^{15}N-Cisplatin (8.5 mg/ml) was dissolved in 0.9% NaCl at 65°C and left at this temperature for 1 h. Lipids (HSPC/cholesterol/^{2000}PEG-DSPE 51:44:5) were dissolved in ethanol. The lipids were hydrated by adding this ethanolic solution to the drug mixture. Final lipid concentration was 150 mg/ml (15%) in 10% ethanol, at 65°C. The mixture was kept stirring for 1 h at 65°C, then extruded at 65°C, 11 times through 200 nm pore size polycarbonate filters using the LiposoFast syringe extruder (Avestin, Ottawa, ON, Canada), followed by extrusion through a 100 nm pore size polycarbonate filter. Sized liposomes (~100 nm) were allowed to cool to room temperature (RT). During the cooling, a heavy yellow precipitate formed. The supernatant was collected and allowed more standing time at room temperature. More precipitation occurred, and the supernatant was collected again. The sample was diluted twofold and dialyzed against 10% sucrose containing 1 mM NaCl, and 5 times against 100 vols. of 10% sucrose containing 1 mM NaCl at room temperature. Under these conditions, a complete equilibration with 10% sucrose containing 1 mM NaCl should occur. Finally, histidine buffer (pH 6.5) was added to a final concentration of 10 mM. The final liposome dispersion was a translucent white. Aliquots of the liposomes and of both precipitates were analyzed by heteronuclear single quantum coherence (HSQC) at 30°C.

2.2.2. Preparation of cisplatin encapsulated in sterically stabilized liposomes (STEALTH cisplatin)

STEALTH cisplatin liposomes (~100 nm) were prepared as described in Section 2.2.1 (except that commercial cisplatin was used). Sample 4 (Table 1) was frozen once and then thawed; both the cisplatin and the liposomes remained intact. Large unilamellar liposomes were prepared containing 99 mg/ml total lipids and 1.64 mg/ml Pt.

2.3. Liposome characterization: analysis of liposome concentration, size and integrity

Liposomes were characterized for their size distribution using photon correlation spectroscopy [20]. Phospholipid concentration was characterized using a modified Bartlett procedure [20]. Lipid degradation was determined using TLC [20,21] and the increase in levels of non-esterified fatty acids [21].

2.4. NMR measurements

2.4.1. ^{195}Pt NMR

^{195}Pt NMR measurements were carried out on a Varian VXR-300S spectrometer having a 7.05 T magnet equipped with a 5 mm computer-switchable probe. The platinum chemical shifts were measured relative to the external reference signal of K_2PtCl_4, set at −1624 ppm. Data were collected with and

without broad-band decoupling of the protons, using a spectral width of 100.0 kHz and acquisition time of 0.010 s. Usually, 350 000 pulses or more were acquired and a line broadening of 300 Hz was applied. The samples were measured, without spinning, at 37°C and 60°C. A capillary containing 2 mg/ml (4.82 mM) K_2PtCl_4 was added to the NMR tubes as an internal reference of a known concentration. The data were apodized using a line broadening equal to the natural line width (in Hz) prior to processing and integration.

2.4.2. ^{31}P NMR

^{31}P measurements were carried out at room temperature and at 60°C using a 5 mm computer-switchable probe. The ^{31}P chemical shifts were measured relative to phosphoric acid set at 0 ppm. Data were collected with broad-band decoupling of the protons, using a spectral width of 10 000 Hz, and an acquisition time of 1.6 s. Usually, 250 pulses or more were acquired and a line broadening of 20.0 Hz was applied. Placebo (control) and cisplatin-loaded liposomes were studied by ^{31}P NMR. The large (~100 nm) unilamellar vesicles (LUV) were composed of hydrogenated phosphatidylcholine (HPC), cholesterol and ^{2000}PEG-DSPE at a mole ratio of 55:40:5. Samples were prepared by mixing 700 μl of the original liposome sample with 70 μl of ^2H_2O.

2.4.3. HSQC NMR measurements

All [^1H, ^{15}N] HSQC data were obtained using a Bruker DXR 400 MHz NMR spectrometer, equipped with a 5 mm multinuclear inverse detection probe. The 2D data were recorded using the Bruker sequence of INVIGSTP (inverse detection 2D ^1H-X correlation via double INEPT transfer, phase sensitive using TPPI with decoupling during acquisition). ^{15}N spins were irradiated during the acquisition time using the GARP-1 sequence. The ^{15}N chemical shifts were externally referenced to 1.5 M NH_4Cl in 1 M HCl ($\delta_N = 0$ ppm, $\delta_H = 7$ ppm); ^1H chemical shifts were externally referenced to TSP (Me_3Si-$(CD_2)_2CO_2Na$) ($\delta_H = 0$ ppm). Two to eight transients were acquired, using an acquisition time of 0.251 s, spectral widths of 2 kHz in both f_2 and f_1 dimensions, and 256 increments of t_1. All spectra were acquired at 300 K (27°C). Spectra were collected in ~20 min. The data were processed using Bruker software, with no line broadening.

2.4.3.1. Sample preparation for HSQC experiments. The ^{15}N-cisplatin (8.5 mg/ml) was dissolved either in 0.9% NaCl or in 10% sucrose, at 65°C. Control samples, without lipids, were prepared and processed according to the same procedures described above for STEALTH cisplatin preparation (see Section 2.2.1). After cooling, histidine buffer (10 mM, pH 6.5) was added. Treated samples were stored at 4°C or −20°C.

2.4.4. Quantification of platinum content by ^{195}Pt NMR

K_2PtCl_4 was chosen as an internal reference since it is a stable compound whose chemical shift (−1624 ppm) is in close proximity to that of cisplatin (−2100 ppm), yet is distant enough to avoid overlapping. The K_2PtCl_4 (2 mg/ml, 4.82 mM), was sealed in a glass capillary, and concentrated HCl was added to prevent its hydrolysis. The capillary was inserted into the 5 mm NMR tube containing the sample, and the

Table 1
Liposomal formulations used for ^{195}Pt NMR spectroscopy

Parameter	Sample 1	Sample 2	Sample 3	Sample 4
Size (nm)	112	125	100	107
cis-DDP (mg/ml)	1.0	1.0	0.9	0.9
Lipid (mM)	104	89	110	110
Linewidth (Hz, 37°C)	848.08	844.51	789.40	797.53
Linewidth (Hz, 60°C)	994.08	1017.44	861.06	868.92
External phase	10% sucrose	0.9% NaCl	3% sucrose	3% sucrose
	1 mM NaCl		3.3% NaCl	3.3% NaCl
	10 mM histidine	10 mM histidine	10 mM histidine	10 mM histidine
	pH 6.5	pH 6.5	pH 6.5	pH 6.5

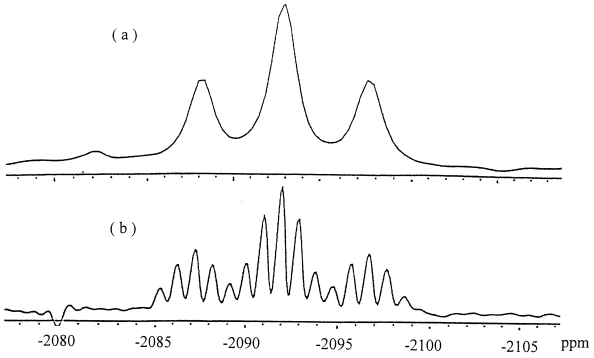

Fig. 2. ^{195}Pt NMR spectra of *cis*-Pt($^{15}NH_3$)$_2$Cl$_2$ (a) with and (b) without broad-band decoupling.

^{195}Pt NMR spectrum was acquired as described above.

To test the method's accuracy, three cisplatin samples of varying concentrations (1.54, 2.0 and 2.31 mg/ml) were measured in the presence of the capillary at 37°C. The areas under the curves were integrated relative to the area under the reference peak, and the elemental platinum concentration was calculated. To verify the calculated concentrations, AAS was performed.

2.5. Atomic absorption spectroscopy

Atomic absorption measurements were performed on a Varian SpectrAA Zeeman 300 spectrometer. The platinum concentration was calculated according to a calibration curve of a known concentration of a K_2PtCl_4 stock solution (250 ng/ml, 6.02×10^{-4} mM).

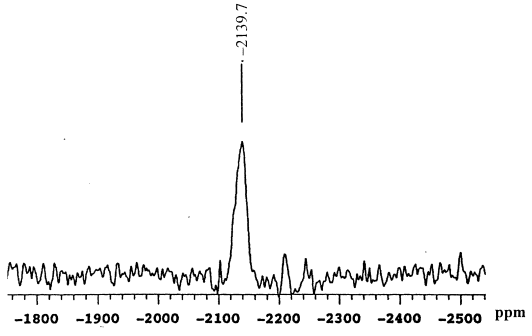

Fig. 3. ^{195}Pt NMR spectrum of cisplatin encapsulated in liposomes.

3. Results

3.1. Analysis by ^{195}Pt NMR

3.1.1. ^{195}Pt NMR of ^{15}N-labeled cisplatin

cis-Pt($^{15}NH_3$)$_2$Cl$_2$ was prepared (see Section 2.1) and characterized by ^{195}Pt NMR spectroscopy. The broad-band decoupled spectrum shows the expected triplet due to the coupling of two equivalent ^{15}N atoms (Fig. 2a). When the broad-band decoupling was turned off, each of the three ^{195}Pt resonances was split to a septet by the six equivalent hydrogens (Fig. 2b).

3.1.2. ^{195}Pt NMR of cisplatin encapsulated in liposomes

^{195}Pt NMR measurements of liposome-encapsulated cisplatin clearly show a single chemical shift (range −1350 to −2700 ppm) at −2139.7 ppm, indicating mainly (>90%) one species of Pt(II), which is the intact cisplatin (Fig. 3). No additional platinum peaks were detected, indicating that no other platinum species (i.e., platinum tri- or tetra-amine) were formed, though adducts of Pt(II) with large molecules would not be observed by ^{195}Pt NMR.

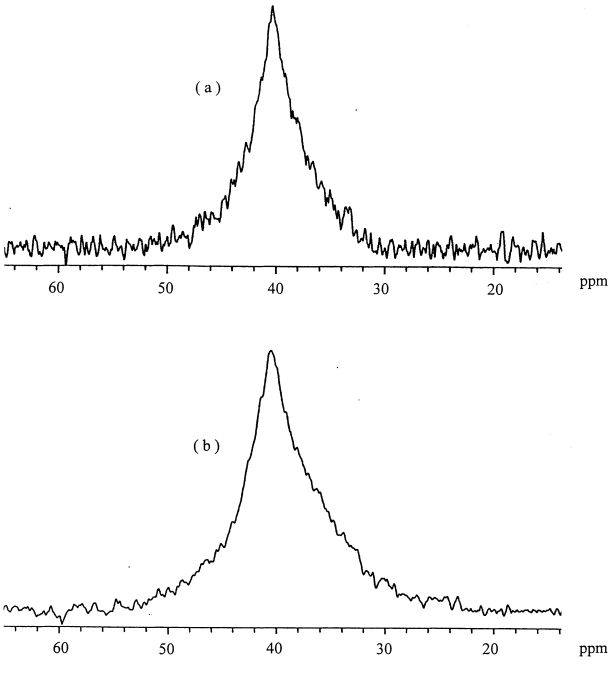

Fig. 4. ^{31}P NMR spectra of (a) cisplatin-containing liposomes and (b) control liposomes.

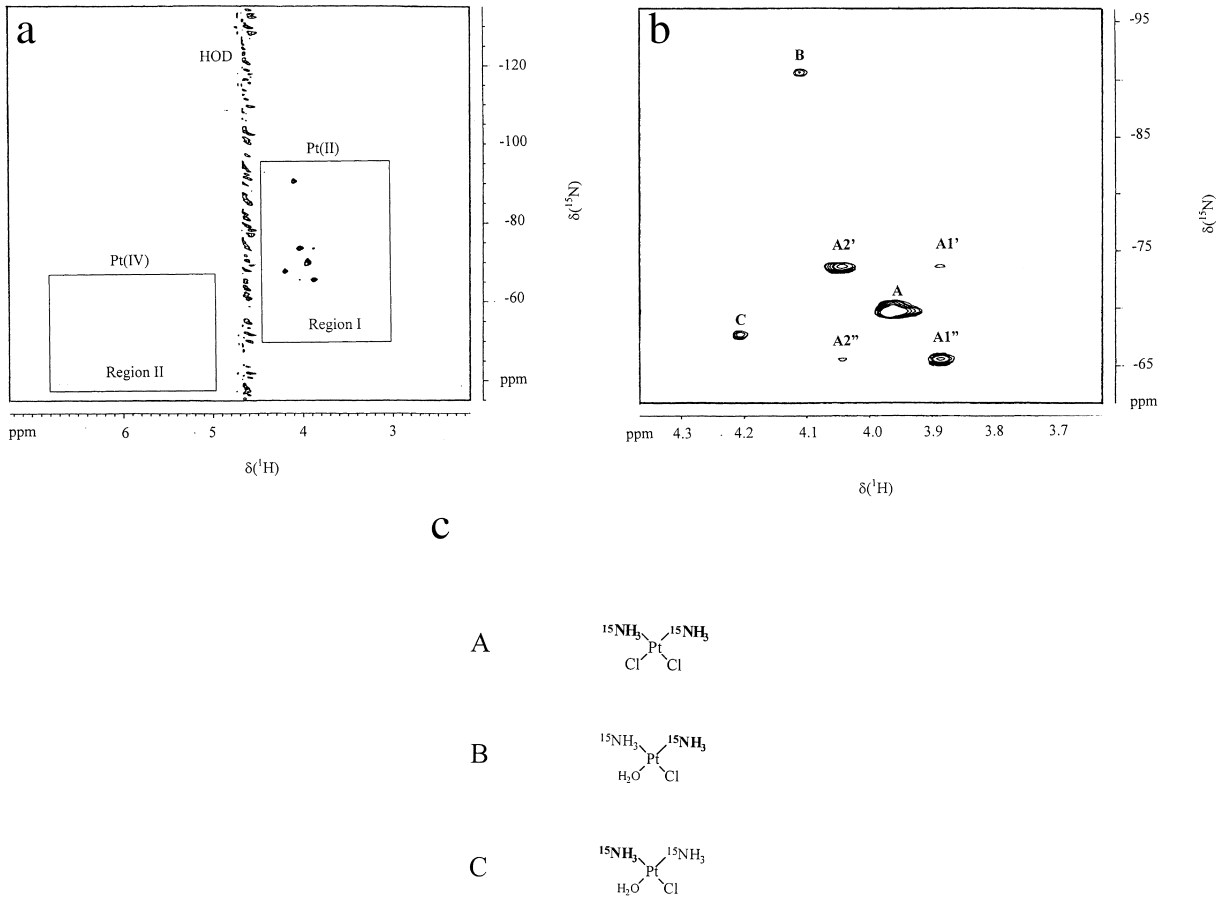

Fig. 5. HSQC spectrum of *cis*-Pt($^{15}NH_3$)$_2$Cl$_2$ in water (a), and (b) an enlargement of region I. (c) Schematic representation of the species detected in the HSQC spectrum of ^{15}N-labeled cisplatin.

Pt(II) can undergo a two-electron disproportionation to give solid Pt(0) and soluble Pt(IV) complexes, especially when they are heated in non-acidic solutions. No black precipitate was detected in the samples, suggesting that no Pt(0) was present, and no peaks were observed in the ^{195}Pt NMR in the region between +1000 and −500 ppm, indicating that no Pt(IV) complexes were present in the liposomal dispersion.

3.2. Analysis by ^{31}P NMR

The ^{31}P NMR spectra of the liposome formulations described in Table 2 were measured; they displayed the slightly asymmetric peaks typical of phospholipid vesicles. The same samples were measured by ^{195}Pt NMR to verify their platinum content. At room temperature, the ^{31}P peak observed was very broad. This is in agreement with previous data of vesicles composed of saturated phospholipids and cholesterol in their liquid ordered phase, below the gel-to-liquid crystalline phase transition temperature (T_m) of the matrix lipids (T_m = 52.5°C for HPC) [22]. At 60°C (above T_m for HPC), sharp spectra were obtained for both the control and platinum-containing liposomes. At 60°C, ~10 scans were sufficient to produce reliable data with high signal-to-noise ratio (Fig. 4). Peak analysis revealed somewhat asymmetric peaks for both (skewness to the right), as is expected for phospholipid vesicles. Measurement of the linewidths at half the height can serve as a criterion for the interaction of the platinum with the phospholipids in the formulation. Linewidths at half the height ($\Delta\nu_{1/2}$) were determined at 60°C, and values of 6.3 ppm and 4.2 ppm were obtained for the control and the cisplatin liposomes, respectively.

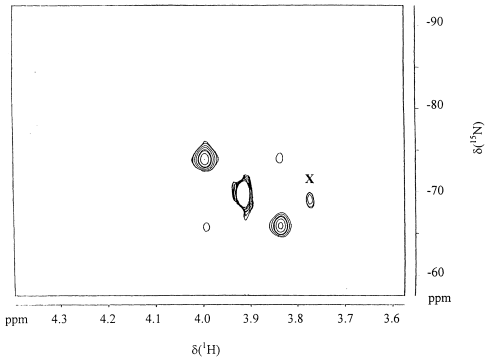

Fig. 6. HSQC spectrum of *cis*-Pt($^{15}NH_3$)$_2$Cl$_2$ encapsulated in the liposomes; the peak denoted as 'X' is unidentified.

3.3. Analysis by HSQC

In a typical HSQC experiment we were able to observe micromolar concentrations of cisplatin in ~20 min. In addition to the tremendous gain in sensitivity, HSQC selectively detects only the protons that are coupled to the ^{15}N, thus ignoring all the other protons in the solution (from the liposomes) and simplifying the interpretation of the data. For an overview of ^{1}H-^{15}N-HSQC NMR, see Section 4.2.

3.3.1. HSQC of ^{15}N-labeled cisplatin in water

The HSQC of *cis*-Pt($^{15}NH_3$)$_2$Cl$_2$ in water is depicted in Fig. 5. The correlation peaks are located in region I, which is characteristic of Pt(II) complexes. There are no peaks in region II, where the Pt(IV) peaks are expected. An enlargement of region I (Fig. 5b) shows that there are three peaks (A, B and C) and each peak has additional satellites (A1′, A1″, A2′ and A2″). The satellites result from the spin-spin coupling between the ^{195}Pt (33% natural abundance) and the protons/^{15}N [23]. Peak A belongs to *cis*-Pt($^{15}NH_3$)$_2$Cl$_2$, where the two equivalent nitrogens give rise to a single peak. Peaks B and C belong to a single complex of *cis*-[Pt($^{15}NH_3$)$_2$Cl(H$_2$O)]$^+$, where peak B is ascribed to the nitrogen that is *trans* to the aqua ligand, and peak C to the nitrogen that is *trans* to the chloride ligand (Fig. 5c). The ^{195}Pt-^{15}N coupling constants can be measured from the distance between A1′ and A1″, and the ^{195}Pt-^{1}H coupling constants can be measured from the distance between A1″ and A2″. The hydrolysis reaction of cisplatin in aqueous solutions is not easily observed by ^{195}Pt NMR, but is easily observed by HSQC. The results obtained here are consistent with those reported in the literature [23] (J(^{1}H-^{195}Pt) ~64 Hz, J(^{15}N-^{195}Pt) ~320 Hz).

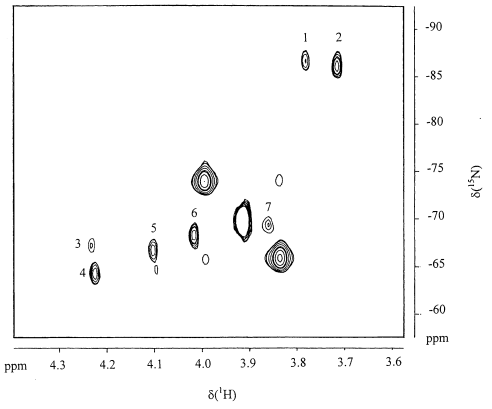

Fig. 7. HSQC spectrum of *cis*-Pt($^{15}NH_3$)$_2$Cl$_2$ following encapsulation in the presence of a histidine buffer; peaks 1–7 are attributed to *cis*-Pt($^{15}NH_3$)$_2$Cl$_2$-histidine species.

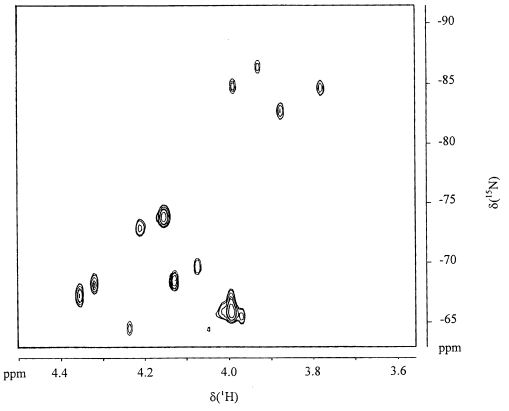

Fig. 8. HSQC spectrum of cisplatin following incubation with *N*-acetylhistidine.

3.3.2. HSQC of ^{15}N-labeled cisplatin encapsulated in liposomes

HSQC spectra of *cis*-Pt($^{15}NH_3$)$_2$Cl$_2$ passively encapsulated in the aqueous phase of ~100 nm LUV appear almost identical to the spectrum of the free drug. Buffers, such as histidine, were added after the encapsulation was complete, and all excess drug was removed. However, there is one small difference between the spectral details of the HSQC of the ^{15}N-labeled cisplatin in water and in the liposomes: the distance between the satellite peaks in the ^{15}N liposomal cisplatin is somewhat smaller than in the non-encapsulated compound. The spectrum does not dis-

Table 2
Liposomal formulations used for ^{31}P and ^{195}Pt NMR spectroscopy

	P (mg/ml)	Phospholipids (mM)	Total lipids (mg/ml)	Pt (mg/ml)	Size[a] (nm)	$\Delta\nu_{1/2}$ (60°C) (ppm)
Control-SSL	2.65	86	109	–	104	6.3
Cisplatin-SSL	9.75	315	403	1.8	116	4.2

[a]All size distributions were unimodal, S.D. did not exceed 15%.

play any peaks in the Pt(IV) region, indicating that the process of encapsulation of *cis*-Pt($^{15}NH_3$)$_2$Cl$_2$ into the liposomes did not cause disproportionation of the cisplatin (Fig. 6). In addition, the lack of a $^{15}NH_4^+$ peak in the spectrum suggests that no deamination (loss of the ^{15}N ligand) occurred and that all the Pt(II) complexes can be accounted for by the HSQC experiment. Visible in the spectrum are the expected cisplatin peaks, as well as an unidentified peak (marked X); HPLC chromatograms of these samples detected only very minor impurities ($<5\%$) (results not shown).

3.3.3. HSQC of ^{15}N-labeled cisplatin encapsulated in liposomes in the presence of a histidine buffer

The ^1H-^{15}N-HSQC spectra revealed peaks additional to those of the ^{15}N-labeled compound after exposing the ^{15}N-labeled drug to histidine (Fig. 7). Further experiments in which the ^{15}N-cisplatin was exposed to known quantities of histidine during liposome preparation indicated that these foreign peaks could be attributed to binding of the drug to the histidine in the buffer during the encapsulation process. We chose to test the reactivity of the ^{15}N-labeled cisplatin towards biological buffers. Protected *N*-acetylhistidine was used in order to eliminate the contribution of the histidine amino group. Following 24 h incubation of a 1:1 mole ratio of ^{15}N-cisplatin and *N*-acetylhistidine, various new peaks appeared, probably belonging to cisplatin-histidine species (Fig. 8). These results were further verified by means of HPLC; the chromatograms obtained indeed verified the presence of a cisplatin-histidine species ($\sim$20–30% of the platinum detected) (results not shown). No additional peaks were detected when the ^{15}N-cisplatin was loaded into the liposomes in the absence of histidine or when histidine was added after the unencapsulated drug was removed (see Section 2.2.1). Similar results were obtained when *N*-BOC-methionine was incubated for 24 h in the presence of ^{15}N-cisplatin, at a 1:1 mole ratio.

3.4. Solubility studies

3.4.1. Visual precipitation studies

Visual assessment showed that the solubility of cisplatin is temperature dependent. At 4°C, 1 mg/ml cisplatin was completely soluble; at 37°C, 2 mg/ml; at 65°C, 8 mg/ml. No yellow precipitation of cisplatin was detected in any of these cases.

3.4.2. Solubility studies in the aqueous phase and in the presence of ethanol

We compared the solubility of cisplatin at 1 and 8 mg/ml at room temperature and at 65°C (which are the relevant temperatures for encapsulation of the

Table 3
Quantification of cisplatin content by NMR and AAS

Weighed *cis*-DDP (mg/ml)	*cis*-DDP calculated by AA (mg/ml)	*cis*-DDP calculated by NMR (mg/ml)	
		18°C	37°C
1.5	1.5	1.4	1.4
2.0	2.0	1.8	1.8
2.3	2.3	2.1	2.1
5.1[a]	3.7[b]	2.1	3.2

[a]At 60°C, all 5.1 mg/ml *cis*-DDP could be quantified by ^{195}Pt NMR.
[b]Only 3.7 mg/ml of *cis*-DDP is accounted for, since some precipitation occurs during the AA measurement, carried out at room temperature.

Table 4
^{195}Pt NMR linewidths at half the height measured for 2 mg/ml cisplatin in the presence of ^{2000}PEG

^{2000}PEG concentration (%)	Linewidth (Hz)
0	939.351
5	759.275
10	604.318
20	498.031
40	283.973

drug in liposomes) in 0.9% NaCl and in 20% ethanol in 0.9% NaCl. At 1 mg/ml, cisplatin was soluble under all conditions. At 8 mg/ml, most of the cisplatin precipitated at room temperature, but most was soluble at 65°C. Heating, followed by a decrease to room temperature, led to the precipitation of most of the 8 mg/ml of the cisplatin which was dissolved at 65°C, in both the absence and presence of 20% ethanol.

3.5. Quantification of cisplatin content by ^{195}Pt NMR

The level of cisplatin in different liposome preparations was quantified using ^{195}Pt NMR spectroscopy and AAS. The platinum content measured by NMR was verified by AAS (Table 1).

3.6. Effect of ^{2000}PEG on solubility and linewidth of cisplatin as measured by ^{195}Pt NMR

3.6.1. Effect of ^{2000}PEG on solubility of cisplatin

The experiment was carried out at room temperature to isolate the effect of the ^{2000}PEG and exclude the contribution of a rise in temperature. Solubility was studied using both visual precipitation and ^{195}Pt NMR measurements (see Sections 3.4 and 2.4.1). Cisplatin, 5 mg/ml, was dissolved in the presence of increasing concentrations of ^{2000}PEG (10%, 20% and 40% ^{2000}PEG). In the presence of 40% ^{2000}PEG, solubility was achieved fastest. Ten percent ^{2000}PEG had almost no effect on the solubility at RT, as the integrated peak observed was equivalent to ~2.1 mg/ml cisplatin, which is the established solubility of cisplatin at this temperature. Increasing the concentration of ^{2000}PEG up to 40% increased the solubility of cisplatin at RT by ~60%, reaching ~3.3 mg/ml, as observed by NMR. The insoluble cisplatin precipitated as a yellow solid at the bottom of the NMR test tubes.

3.6.2. Effect of ^{2000}PEG on the linewidth of the cisplatin peak in ^{195}Pt NMR

Table 4 shows the effect of increasing the concentration of ^{2000}PEG on the linewidth of the cisplatin peak. The experiment was carried out at room temperature to isolate the effect of the ^{2000}PEG and exclude the contribution of a rise in temperature. It was found that as the ^{2000}PEG concentration increased, the linewidth decreased.

4. Discussion

In order to reach tumor sites in a therapeutically significant way, liposomal formulations must have a sufficient and stable drug load, as well as long circulation time. The liposomes should be small enough (~100 nm) so that they can extravasate into the tumor tissue [15,16,24]. A size of ~100 nm imposes a limitation on the drug loading, especially when it is passive. The solubility of the drug is limited, and the drug has low affinity to the lipid membrane. To improve the drug-to-lipid ratio, drug loading was performed at high temperatures (60–65°C), at which the drug solubility is ~8 mg/ml (4-fold higher than at room temperature). On completion of the preparation of loaded LUV, the temperature was lowered to 4°C, a temperature at which the drug solubility is limited to ~1 mg/ml. This preparation, in which the drug concentration exceeds its solubility by 8-fold, raised a question regarding the physical state of the drug and its stability inside the liposomes during storage at 4°C. Another important question is related to the drug-lipid interaction: if and how the liposome formulation affects the drug and, in turn, how the drug affects the liposomes. Through the application of various NMR techniques, including ^{195}Pt, ^{1}H-^{15}N-HSQC and ^{31}P NMR, we were able to gather information in an attempt to answer these questions.

4.1. Effect of cisplatin on liposome lipids

^{31}P NMR was used to verify the state of phospholipids in vesicle membranes as well as to verify the

homogeneity of liposomal preparations with respect to size distribution and number of lamellae [22,25,26]. Comparison between the cisplatin-containing LUV and the control, cisplatin-free LUV shows that they differ, although both liposome preparations have identical lipid concentration and similar size distribution (see Table 2). This suggests at least minor interactions between the cisplatin and the phospholipid, as $\Delta\nu_{1/2}$ Pt-liposomes (4.2 ppm) $< \Delta\nu_{1/2}$ control (6.3 ppm). The linewidth data are in good agreement with many previously reported ^{31}P measurements of 100–200 nm diameter LUV (i.e., $\Delta\nu_{1/2} \approx 5$ ppm for egg PC/DSPG, 85:15) [26]. Such linewidths suggest lack of contamination with MLV, while the shape of the peaks clearly shows that there are no phospholipids in a hexagonal type II state [26]. Factors such as the vesicle size, the grafted PEG moiety or the presence of ethanol are ruled out as an explanation for the difference in $\Delta\nu_{1/2}$ since they are present and similar in both the cisplatin-free and the cisplatin-containing formulations. Therefore, it is likely that a direct or indirect interaction between the drug and the phospholipids, as well as the effect on hydration due to the preferential distribution of cisplatin in the PEG layer near the phospholipid head group (see Section 4.3), are responsible for the differences in $\Delta\nu_{1/2}$. Further experiments are necessary in order to clarify the nature of this interaction.

4.2. *Effect of liposomal encapsulation on the chemical stability of cisplatin*

^{195}Pt NMR spectroscopy provides information on the oxidation state of the metal and on the nature of the four ligands in platinum's first coordination sphere. This is due to the fact that the chemical shift range of Pt complexes spans several thousand ppm and that the chemical shift is sensitive to both the oxidation state of the Pt (II and IV) and to the nature of the atom which is bound to the Pt. ^{195}Pt NMR is considered one of the most powerful tools for characterizing platinum complexes. The drawbacks of platinum NMR stem from the low natural abundance of the 195 isotope (33%) and from the chemical shift anisotropy (CSA) relaxation pathway of the Pt complexes. The quadrupole moment of the ^{14}N ligand causes the peaks to broaden such that the peak width at half-height ($\omega_{1/2}$) for K_2PtCl_4 is $\sim$50 Hz, for $Pt(NH_3)_2Cl_2$ it is $\sim$200 Hz; while for $Pt(NH_3)_4$ it is $\sim$1150 Hz. The broadening of the peaks masks any information about couplings to the nitrogen ligands (and to the protons) and reduces the signal-to-noise ratio of the spectrum. Moreover, ^{195}Pt NMR spectroscopy cannot be used to study the binding of Pt complexes to biopolymers since the slow rotational correlation time will broaden the peaks beyond detection.

While ^{195}Pt NMR spectroscopy provides information on the oxidation state of the Pt complex and on the nature of atoms in the first coordination sphere, it cannot distinguish between a water ligand, a carboxy ligand or a phosphate ligand, since they all bind the Pt through an oxygen atom. ^{15}N NMR spectroscopy has been used in conjunction with ^{195}Pt NMR spectroscopy to provide the missing information [23,27]. The ^{15}N chemical shift and the ^{15}N-^{195}Pt coupling constants are sensitive to the ligand that is *trans* to the ^{15}N [28]. The lack of ^{14}N causes the ^{195}Pt resonance to be sharp, and the coupling constants (^{195}Pt-^{15}N, ^{195}Pt-^{1}H) can be obtained. While it is easy to prepare ^{15}N-labeled cisplatin (*cis*-$Pt(^{15}NH_3)_2Cl_2$), direct detection of the ^{15}N nucleus is difficult due to its low sensitivity.

Inverse detection experiments circumvent the above-mentioned problem by detecting the protons that are coupled to ^{15}N. This two-dimensional technique provides information about the chemical shifts and coupling constants of the ^{15}N, which depend on the ligands in the first coordination sphere of the Pt, and on its oxidation state. The main advantage of using ^{15}N-labeled cisplatin is the ability to apply heteronuclear single or multiple quantum coherence (HSQC or HMQC) NMR techniques. HSQC and HMQC are two-dimensional inverse detection methods that have the proton chemical shifts on one axis and the ^{15}N chemical shifts on the second axis. HSQC and HMQC of ^{15}N-labeled Pt complexes have been used successfully to detect micromolar concentrations of Pt complexes.

The initial formulations with the cisplatin included the addition of a histidine buffer prior to encapsulation in the liposomes. ^{1}H-^{15}N-HSQC NMR is sensitive enough to detect even the slightest impurities in the sample. This was the case with the histidine buffer that was used in the process of platinum encapsu-

lation in the liposomes. It is known that some amino acids, such as histidine and methionine, may react with cisplatin [29]. These associations are irreversible, thus making the drug unavailable and ineffective, once bound. To avoid any inactivation of cisplatin by histidine during the preparation of STEALTH cisplatin, no histidine buffer was added until the encapsulation was completed, and any unencapsulated drug was removed (see Section 3.3.3).

The incubation experiments we have carried out suggest that there is no contact between the histidine buffer and ^{15}N-cisplatin, and that in STEALTH cisplatin, the liposomes do not leak and are very stable. That is, there is no cisplatin associated with the external face of the liposome membrane, and the lack of leakage of the ^{15}N-labeled cisplatin from the liposomes is proven by the fact that peaks belonging to cisplatin-histidine species are not observed.

4.3. Physical state of liposome-encapsulated cisplatin

A very important parameter to be determined regarding the platinum encapsulated in the liposomes is the drug-to-lipid ratio, and what fraction of the liposomal drug is behaving like water-soluble cisplatin. In the case of cisplatin, it is expected that only the soluble portion of the drug within the liposome will be bioavailable to act upon cellular DNA; any cisplatin precipitate may be considered as unavailable and ineffective. The comparative study we have carried out indicated that, unlike atomic absorption spectroscopy, it was possible to use ^{195}Pt NMR measurements in order to selectively quantify the soluble cisplatin (see Table 3) and thus obtain a clear indication as to the physical states of the cisplatin contained in the liposomes. Any platinum in the solid state (i.e., in a crystalline state or as a precipitate or even in a suspension of very fine particles) would be undetected by ^{195}Pt NMR, as lines will broaden to such an extent that they would disappear into the baseline.

The agreement between the ^{195}Pt NMR and atomic absorption data for STEALTH cisplatin indicates that nearly all the cisplatin accounted for by atomic absorption is also detected by ^{195}Pt NMR, and is therefore soluble in the intraliposomal aqueous phase. This suggests that at 4°C or at room temperature, the intraliposomal concentration is higher than 1–2 mg/ml, which is the bulk solubility limit at these temperatures. Further, the NMR measurements indicate that the solubility of free cisplatin in the bulk at 18°C in the aqueous phase is limited to $\sim$2 mg/ml, and is increased to at least 8 mg/ml upon a rise in temperature to 60°C. These results are in good agreement with the visual precipitation studies performed (Section 3.4.2). The NMR studies, when combined with the solubility measurements and AAS, led us to conclude that the encapsulated cisplatin does not precipitate in the liposomes. This result is in good agreement with extended X-ray absorption fine structure (EXAFS) analysis performed by Lasic et al. [30]. Since this finding was surprising, it was imperative to try to determine the factors in the preparation that yielded a solubility of cisplatin that is normally obtained only at 65°C.

Ethanol is present during the first stages of liposome formulation, and therefore its effect on the solubility of cisplatin had to be evaluated. The solubility studies performed (Section 3.4.2) led us to conclude that the presence of 20% ethanol did not improve the solubility of cisplatin and is not responsible for the higher than expected drug-to-lipid ratio.

Since ethanol had no effect as an enhancer of cisplatin solubility, other parameters were explored. The contribution of the grafted PEG was studied, since PEG is known to affect solubility in both organic and aqueous media [31–34]. In STEALTH cisplatin, the liposomes consist of 5 mole% ^{2000}PEG-DSPE. This high PEG concentration grafted in proximity to the inner leaflet of the LUV, being in the transition between brush and mushroom configurations, and highly hydrated [35], can contribute to the elevated solubility of cisplatin. Therefore, we have tested the effect of ^{2000}PEG on the solubility of cisplatin by ^{195}Pt NMR and by visual assessment studies. As the concentration of PEG in the solution is increased, the amount of bound water increases accordingly, and the amount of unbound water is decreased. At 40% PEG, most of the water is bound to the PEG (as hydration water [35]). The fact that the solubility of cisplatin increases by some 64% (from 2.1 to 3.3 mg/ml) indicates that cisplatin is soluble in the PEG hydration water and that its solubility in this water is greater than its solubility in bulk water. Therefore, in STEALTH cisplatin, the elevated sol-

ubility of cisplatin suggests that at least part of the cisplatin is found in the bound water layer. In addition, the water structure probably contributes to the correlation time, t_c, as the linewidth ($\Delta\nu_{1/2}$) is reduced with the increase in PEG from ~759 Hz at 5% PEG to ~284 Hz at 40% PEG (see Table 4). The nature of this contribution has yet to be determined, since it would be expected that the opposite would occur. Since elevated concentrations of PEG increase the viscosity of the sample, it would be expected that lines would be broader, whereas the reported results indicate reduced linewidths.

The intraliposomal water includes bulk water and hydration water. For a lipid composition with fixed levels of ^{2000}PEG-DSPE, the liposome's shape and size will determine the ratio between bulk and surface hydration water in the intraliposomal aqueous phase. If a similar shape is assumed, then size alone will be the determining factor. This can be expressed as an area/volume ratio that increases as the liposome size decreases. That is, the smaller the liposomes, the larger is the relative fraction of water associated with the PEG moiety. Therefore, the smaller the liposomes, the higher is the relative solubility of cisplatin in the intraliposomal aqueous phase. Also, the smaller the liposome, the higher is the fraction of cisplatin in the PEG layer. Therefore, $\Delta\nu_{1/2}$ of the liposomal cisplatin should be shorter, as is demonstrated in Table 1. The contribution of the altered water activity with cisplatin is suggested by the HSQC data obtained: (i) The only difference between the spectrum of *cis*-Pt($^{15}NH_3$)$_2$Cl$_2$ passively encapsulated in the aqueous phase of the liposomes and that of the drug in the bulk medium is that the distance between the satellite peaks is somewhat smaller than in the former. (ii) In addition, no peaks attributed to the aqua species are observed. The ^{31}P NMR results described in Section 3.2 and the lack of peaks attributed to the aqua species support the explanation of 'low' average water activity inside the liposomes, compared to the activity of bulk water. This is not surprising, since the internal volume of ~100 nm liposomes is small, and the PEGylated lipid, which binds ~180 mol water/mol ^{2000}PEG moiety [35], reduces the amount of unbound water inside the liposome. The increasing size of the liposome is accompanied by a net decrease in the ratio between the volume of the PEG layer and the internal aqueous volume, as expected from the effect of LUV size on the area/volume ratio.

Other parameters which may explain the improved cisplatin solubility in the intraliposomal aqueous phase of STEALTH cisplatin include the increase of liposome size by swelling and/or shape changes after the liposome preparation was cooled down. The liposome internal aqueous volume may also increase during the cooling process due to a change in liposome shape (i.e., from non-spherical to spherical). Overall, when the liposome size is increased, the fraction of cisplatin present in the intraliposomal unbound water is increased. The observed effect of ^{2000}PEG on the linewidth of the cisplatin peak (Table 4) is in agreement with the inverse correlation between the LUV size and the width of the cisplatin peak observed (Table 1). This phenomenon repeated itself at both 37°C and at 60°C, yet was somewhat more obvious at the higher temperature (Table 1). This suggests a direct or indirect interaction between the PEG moiety of the lipopolymer and cisplatin (probably through water). As the liposome size increases, the amount of unbound water within increases, as there is an increase in the volume per area. This argument further strengthens our suggestion that cisplatin is also found in the bound water within the liposome, although this by itself accounts only for part of the improved solubility, leading to the higher than expected concentration of cisplatin found in the liposomes. It is highly likely that encapsulation in the small internal volume of the liposomes leads to the formation of a special microenvironment which further contributes to the very high drug loading and the higher than expected drug-to-lipid ratio.

5. Conclusions

Our studies on STEALTH cisplatin show that NMR is a powerful tool in the characterization of drug-lipid interactions, the physical state of the drug inside the liposomes, the chemical stability of the drug, and the barrier properties of the liposomes. Several conclusions stem from these NMR studies.

- As long as histidine is added after the drug encapsulation, cisplatin remains intact during the load-

ing process. Encapsulated cisplatin resembles, with minor differences, the parent compound dissolved in the aqueous phase.

- All the cisplatin present in the liposomes behaves like a water-soluble drug, and there is no indication of any insoluble drug. That is, the drug within the liposomes does not precipitate or crystallize.
- Drug-membrane interactions exist but are minimal.
- Drug encapsulated in the liposomes is very stable: no efflux of drug or influx of medium components was observed.
- Improved cisplatin solubility over bulk solubility is explained by the contribution of the membrane-grafted ^{2000}PEG and possibly by the small size of the internal aqueous compartment.

Acknowledgements

This project was supported in part by ALZA Corporation, Mountain View, CA. We would like to acknowledge D. Lasic for sharing his results with us prior to publication. The help of Mr. Sigmund Geller in editing this manuscript is acknowledged with pleasure.

References

[1] B. Rosenberg, L. Van Camp, T. Kirgan, Inhibition of cell division in *Escherichia coli* by electrolysis products from a platinum electrode, Nature 205 (1965) 698–699.

[2] K.M. Comess, S.J. Lippard, Molecular aspects of platinum-DNA interactions, in: S. Neidle, M. Waring (Eds.), Molecular Aspects of Anticancer Drug-DNA Interactions, vol. 1, Macmillan, London, 1993, pp. 134–168.

[3] A.L. Pinto, S.J. Lippard, Binding of the antitumor drug *cis*-diamminedichloroplatinum(II) (cisplatin) to DNA, Biochim. Biophys. Acta 780 (1985) 167–180.

[4] C.A. Lepre, S.J. Lippard, Interaction of platinum antitumor compounds with DNA, Nucleic Acids Mol. Biol. 4 (1990) 3–9.

[5] D. Yang, S.S.G.E. van Boom, J. Reedijk, J.H. van Boom, A.H.-J. Wang, Structure and isomerization of an intrastrand cisplatin-cross-linked octamer DNA duplex by NMR analysis, Biochemistry 34 (1995) 12912–12920.

[6] M. Sip, A. Schwartz, F. Vovelle, M. Ptak, M. Leng, Distortions induced in DNA by *cis*-platin interstrand adducts, Biochemistry 31 (1992) 2508–2513.

[7] S.J. Brown, P.J. Kellert, S.J. Lippard, Ixr1, a yeast protein that binds to platinated DNA and confers sensitivity to cisplatin, Science 261 (1993) 603–605.

[8] U.-M. Ohndorf, M.A. Rould, Q. He, C.O. Pabo, S.J. Lippard, Basis for recognition of cisplatin-modified DNA by high-mobility group proteins, Nature 399 (1999) 708–712.

[9] P. Boffetta, A.M.J. Fichtinger-Schepman, E. Weiderpass, H.C.M. Andijkknijnenburg, G. Stoter, A.T. Vanoosterom, H.J. Keizer, S.D. Fossa, J. Kaldor, P. Roy, Cisplatin-DNA adducts and protein-bound platinum in blood of testicular cancer patients, Anti-Cancer Drugs 9 (1998) 125–129.

[10] C.L. Litterst, A.F. LeRoy, A.M. Guarino, Disposition and distribution of platinum following parenteral administration of cis-dichlorodiammineplatinum(II) to animals, Cancer Treat. Rep. 63 (1979) 1485–1492.

[11] M.P. Hacker, Toxicity of platinum-based anticancer drugs, in: G. Powis, M.P. Hacker (Eds.), The Toxicity of Anticancer Drugs, McGraw-Hill, New York, 1991, p. 82.

[12] G.K. Ogilvie, M.J. Fettman, V.J. Jameson, L.M. Walters, M.H. Lafferty, M.F. Cooper, B.E. Powers, P.A. Ciekot, S.W. Atwater, S.J. Withrow, Evaluation of a one-hour saline diuresis protocol for administration of cisplatin to dogs, Am. J. Vet. Res. 53 (1992) 1666–1669.

[13] V. Pinzani, F. Bressolle, I.J. Haug, M. Galtier, J.P. Blayac, P. Balmes, Cisplatin-induced renal toxicity and toxicity-modulating strategies: a review, Cancer Chemother. Pharmacol. 35 (1994) 1–9.

[14] M.J. McKeage, G. Abel, L.R. Kelland, K.R. Harrap, Mechanism of action of an orally administered platinum complex [ammine bis butyrato cyclohexylamine dichloroplatinum (IV) (JM221)] in intrinsically cisplatin-resistant human ovarian carcinoma in vitro, Br. J. Cancer 69 (1994) 1–7.

[15] A. Gabizon, R. Catane, B. Uziely, B. Kaufman, T. Safra, R. Cohen, F. Martin, A. Huang, Y. Barenholz, Prolonged circulation time and enhanced accumulation in malignant exudates of doxorubicin encapsulated in polyethylene-glycol coated liposomes, Cancer Res. 54 (1994) 987–992.

[16] A. Gabizon, Y. Barenholz, Liposomal anthracyclines: from basics to clinical approval of PEGylated liposomal doxorubicin, in: A.S. Janoff (Ed.), Liposomes: Rational Design, Marcel Dekker, New York, 1999, pp. 343–362.

[17] P.K. Working, M.S. Newman, T. Sullivan, M. Brunner, M. Podell, Z. Sahenk, N. Turner, Comparative intravenous toxicity of cisplatin solution and cisplatin encapsulated in long-circulating pegylated liposomes in cynomolgus monkeys, Toxicol. Sci. 46 (1998) 155–165.

[18] M.S. Newman, G.T. Colbern, P.K. Working, C. Engbers, M.A. Amantea, Comparative pharmacokinetics, tissue distribution, and therapeutic effectiveness of cisplatin encapsulated in long-circulating, pegylated liposomes (SPI-077) in tumor-bearing mice, Cancer Chemother. Pharmacol. 43 (1999) 1–7.

[19] C.S. Boreham, J.A. Groohead, D.P. Fairlie, A ^{195}Pt and ^{15}N N.M.R. study of the anticancer drug, *cis*-diamminedichloroplatinum(II), and its hydrolysis and oligomerization products, Aust. J. Chem. 34 (1981) 659–669.

[20] Y. Barenholz, S. Amselem, Quality control assays in the development and clinical use of liposome-based formulations, in: G. Gregoriadis (Ed.), Liposome Technology, 2nd edn., vol. I, Liposome Preparation and Related Techniques, CRC Press, Boca Raton, FL, 1993, pp. 527–616.
[21] D. Simberg, D. Hirsch-Lerner, R. Nissim, Y. Barenholz, Comparison of different commercially-available cationic lipid-based transfection kits, J. Liposome Res. 10 (2000) 1–13.
[22] D. Lichtenberg, Y. Barenholz, Liposomes: preparation, characterization, and preservation, in: D. Glick (Ed.), Methods of Biochemical Analysis, vol. 33, Wiley, New York, 1998, pp. 337–462.
[23] K.J. Barnham, S.J. Berners-Price, Z. Guo, P. del Socorro, P. Murdoch, P.J. Sadler, NMR spectroscopy of platinum drugs: from DNA to body fluids, in: H.M. Pinedo, J.H. Schornagel (Eds.), Platinum and Other Metal Coordination Compounds in Cancer Chemotherapy 2, Plenum Press, New York, 1996, pp. 1–16.
[24] Y. Barenholz, Design of liposome-based drug carriers: from basic research to application as approved drugs, in: D.D. Lasic, D. Papahadjopoulos (Eds.), Medical Applications of Liposomes, Elsevier Science, Amsterdam, 1998, pp. 541–565.
[25] P.B. Fenske, Structural and motional properties of vesicles as revealed by nuclear magnetic resonance, Chem. Phys. Lipids 64 (1993) 143–162.
[26] C.P.S. Tilcock, Lipid polymorphism, Chem. Phys. Lipids 40 (1986) 109–125.
[27] S.J. Berners-Price, U. Frey, J.D. Ranford, P.J. Sadler, Stereospecific hydrogen-bonding in mononucleotide adducts of platinum anticancer complexes in aqueous solution, J. Am. Chem. Soc. 115 (1993) 8649–8659.
[28] T.G. Appleton, J.R. Hall, S.F. Ralph, ^{15}N and ^{195}Pt NMR spectra of platinum ammine complexes: *trans*- and *cis*-influence series based on ^{195}Pt-^{15}N coupling constants and ^{15}N chemical shifts, Inorg. Chem. 24 (1985) 4685–4693.
[29] N. Farrell, T.G. Appleton, Y. Qu, J.D. Roberts, A.P. Soares Fontes, K.A. Skov, P. Wu, Y. Zou, Effects of geometric isomerism and ligand substitution in bifunctional dinuclear platinum complexes on binding properties and conformational changes in DNA, Biochemistry 34 (1995) 15480–15486.
[30] I. Arcon, A. Kodre, R.M. Abra, A. Huang, J.J. Vallner, D.D. Lasic, EXAFS study of cisplatin in sterically stabilized liposomes, (2000) submitted for publication.
[31] S. Zalipsky, Functionalized poly(ethylene glycol) for preparation of biologically relevant conjugates, Bioconjugate Chem. 6 (1995) 150–165.
[32] G.M. Powell, Polyethylene glycol, in: R.L. Davidson (Ed.), Handbook of Water Soluble Gums and Resins, vol. 18, McGraw-Hill, New York, 1980, pp. 1–31.
[33] M. Mutter, E. Bayer, The liquid-phase method for peptide synthesis, in: E. Gross, J. Meienhofer (Eds.), The Peptides, Academic Press, New York, 1979, pp. 285–332.
[34] G. Karlstrom, O. Engvist, Theory of poly(ethylene glycol) in solution, in: J.M. Harris, S. Zalipsky (Eds.), Poly(ethylene glycol) Chemistry and Biological Applications, American Chemical Society, Washington, DC, 1997, pp. 16–30.
[35] O. Tirosh, Y. Barenholz, J. Katzhendler, A. Priev, Hydration of polyethylene glycol-grafted liposomes, Biophys. J. 74 (1998) 1371–1379.